

Electronic Supporting Information

for

Room Temperature Synthesis of Aqueous Soluble Covellite CuS Nanocrystals with High Photothermal Conversion

Wenhui Chen^a, Yi Xie^{a*}, Chao Hu^a, Tao Zeng^{a,b*}, Huirong Jiang^c, Fen Qiao^d, Jiani Gu^a, Xunyi Dong^a,
Xiujian Zhao^a

^a *State Key Laboratory of Silicate Materials for Architectures, Wuhan University of Technology (WUT), No. 122, Luoshi Road, Wuhan 430070, P. R. China*

^b *School of Materials Science and Engineering, Jingdezhen Ceramic Institute (Xianghu Campus), Xianghu Road, Jingdezhen, Jiangxi 333403, P.R. China*

^c *State Key Laboratory of Advanced Technology for Materials Synthesis and Processing, Wuhan University of Technology (WUT), No. 122, Luoshi Road, Wuhan 430070, P. R. China*

^d *School of Energy & Power Engineering, Jiangsu University, Zhenjiang, 212013, P. R. China*

Email: xiey@whut.edu.cn; zengtao19830823@163.com

Contents

1. Synthesis of Cu_{2-x}S NCs by reacting CuCl_2 with Na_2S in the presence of MPA	3
2. Characterization of Cu_{2-x}S NCs synthesized by reacting CuCl_2 with Na_2S in the presence of TGA	6
3. Characterization of Cu_{2-x}S NCs achieved by reacting CuCl_2 with Na_2S in the presence of GSSG or GSH as ligand.....	8
4. Cu_{2-x}S NCs achieved by reacting $\text{Cu}(\text{NO}_3)_2$ with Na_2S in the presence of various ligands	11
5. XRD patterns and optical spectra of CuS NCs collected by reacting various copper precursors with $(\text{NH}_4)_2\text{S}$	133
6. Gram-scale synthesis of CuS NCs	14
7. Photothermal performance of Cu_{2-x}S NCs.....	155
References.....	18

1. Synthesis of Cu_{2-x}S NCs by reacting CuCl_2 with Na_2S in the presence of MPA

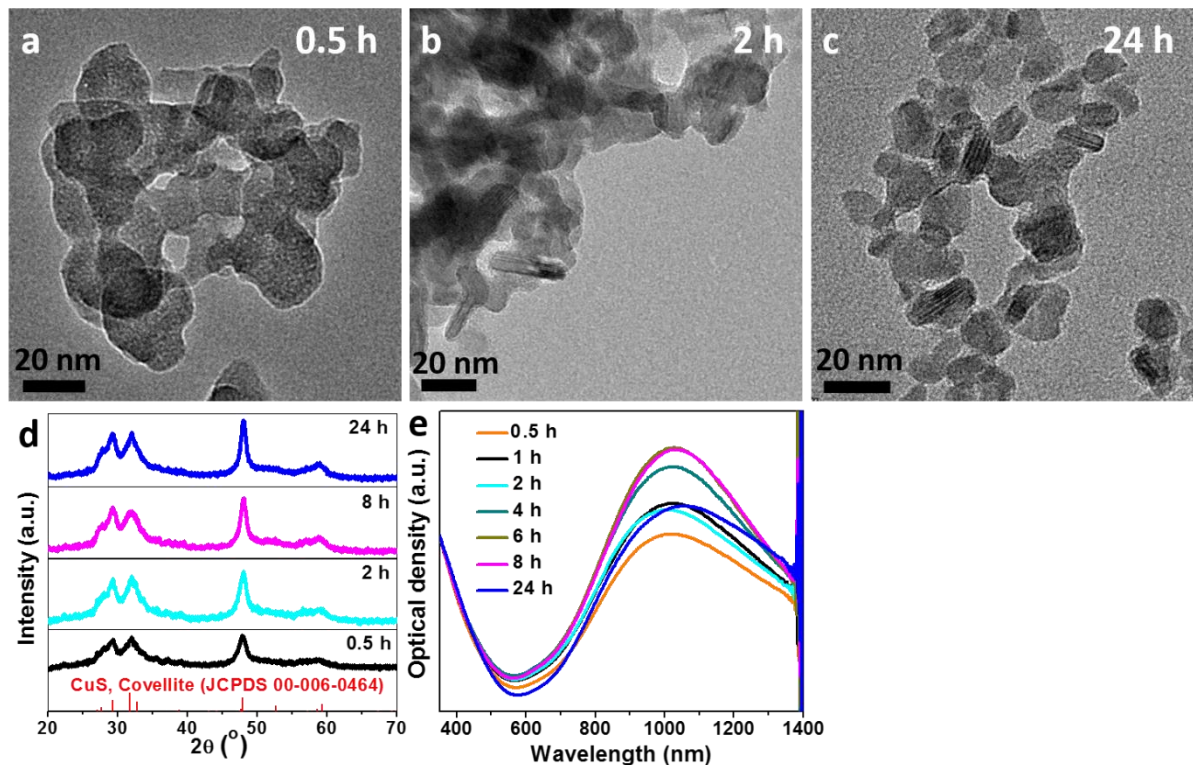


Fig. S1 TEM images (a-c), XRD patterns (d), and optical absorption (e) of CuS NCs collected at different reaction time at room temperature in the presence of MPA. The NCs collected at different reaction time by fixing the precursor S:Cu as 2:1 are plate-like covellite CuS. All the samples display well-defined NIR plasmon absorbance.

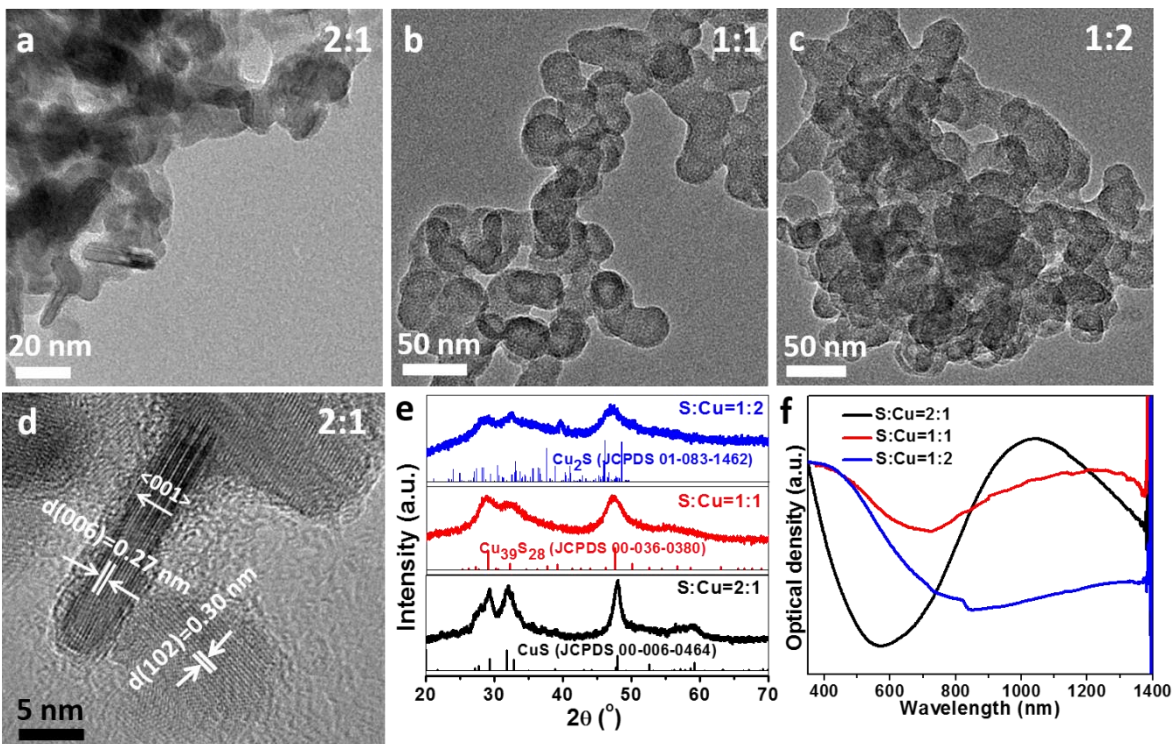


Fig. S2 (a-d) Representative TEM (a-c) and HRTEM images (d) of Cu_{2-x}S NCs achieved with different precursor S:Cu ratios as dictated, at room temperature in the presence of MPA. (e-f) Experimental XRD patterns (e) and optical spectra (f) of the corresponding NCs. For comparison, the standard XRD patterns of covellite (JCPDS No. 00-006-0464), spionkopite ($\text{Cu}_{39}\text{S}_{28}$, JCPDS No. 00-036-0380) and monoclinic low chalcocite (Cu_2S , JCPDS No. 01-083-1462) are provided in panel e). As shown in panels e-f), the precursor S:Cu ratios play a critical role in controlling the structure and the optical properties of the final samples, as evidenced by the evolution of XRD patterns and optical spectra. The NIR plasmon absorbance damped and vanished with decreasing the precursor S:Cu molar ratios.

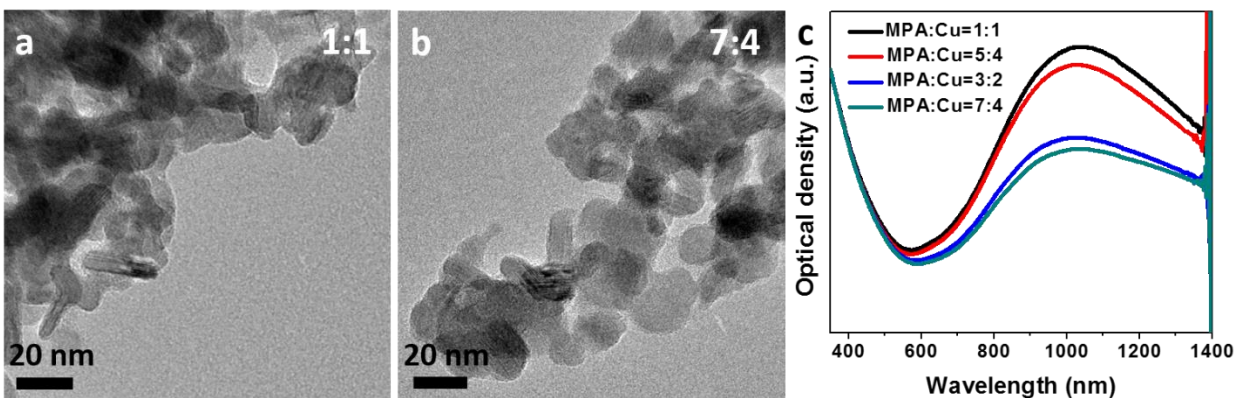


Fig. S3 TEM images (a-b) and optical spectra (c) of CuS NCs synthesized with different starting MPA:Cu ratios as dictated.

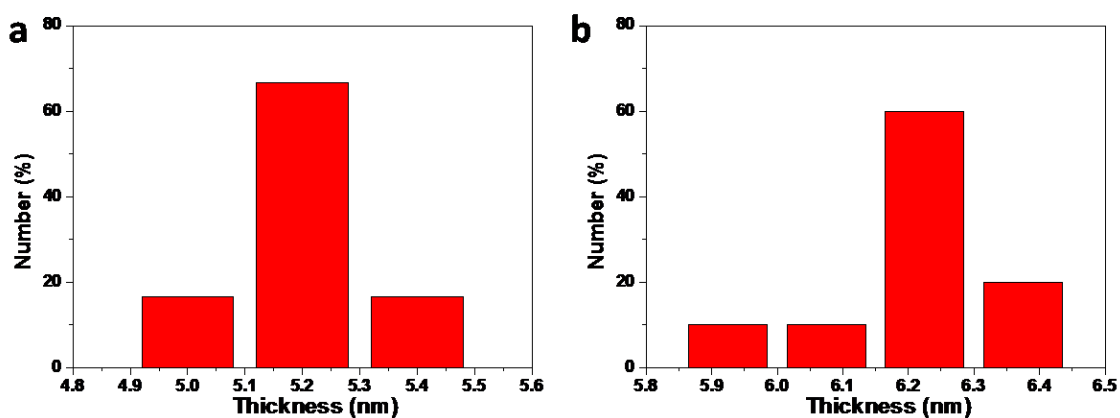


Fig. S4 Size (in thickness) distribution histogram for the CuS nanoplates obtained by reacting CuCl_2 with Na_2S in the presence of MPA for 2 h (a) and 24 h (b), respectively. The average thicknesses of the two typical samples are calculated to be 5.2 ± 0.1 nm, 6.2 ± 0.2 nm, respectively.

2. Characterization of Cu_{2-x}S NCs synthesized by reacting CuCl_2 with Na_2S in the presence of TGA

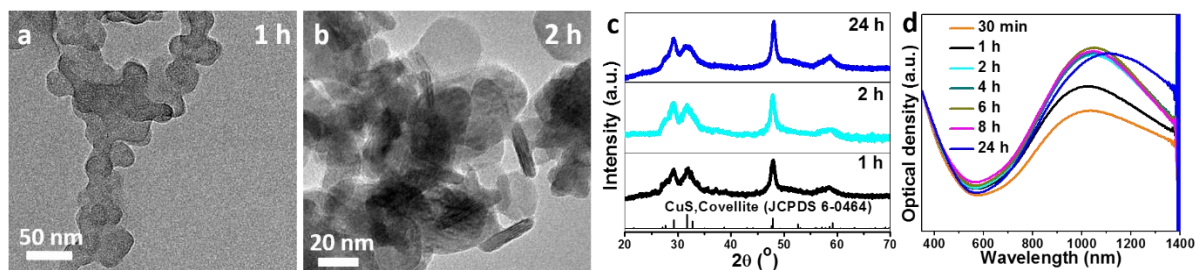


Fig. S5. TEM images (a-b), XRD patterns (c), and optical spectra (d) of CuS NCs collected at different reaction time in the presence of TGA.

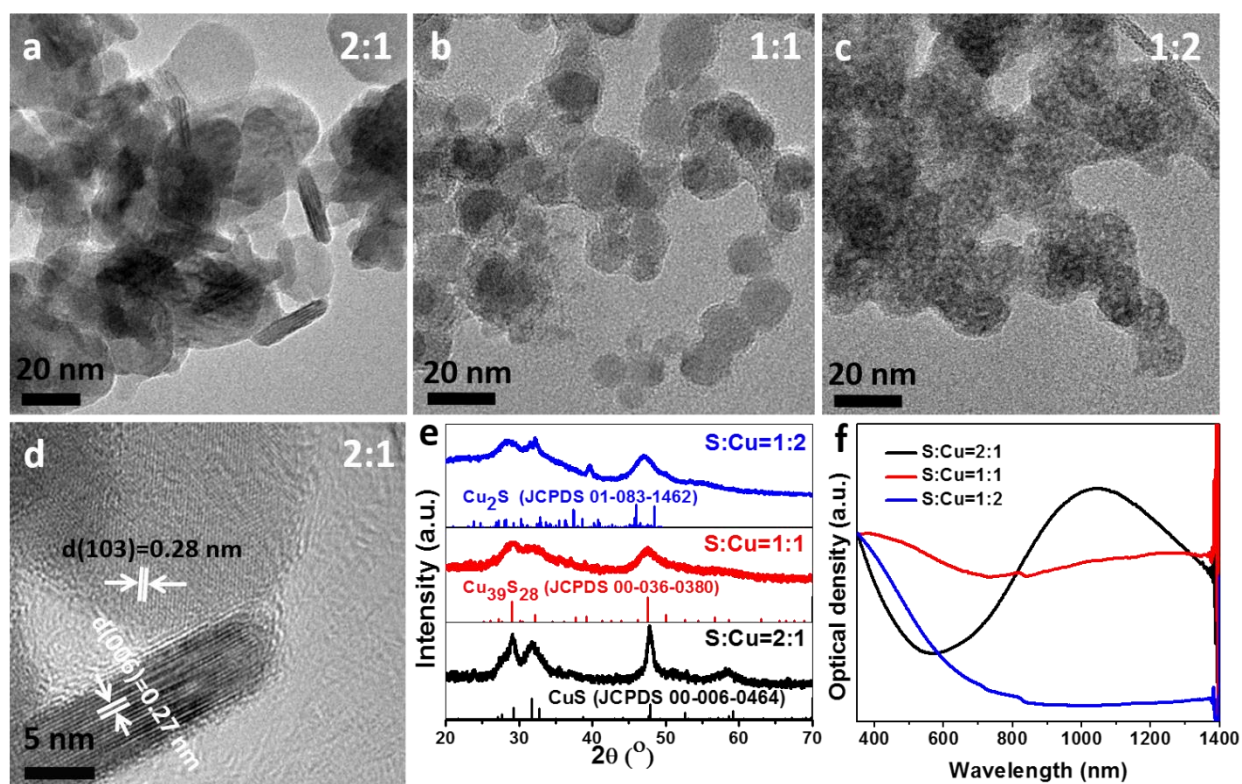


Fig. S6 (a-c) Representative TEM images of Cu_{2-x}S NCs collected with different precursor S:Cu ratios as dictated, in the presence of TGA as ligand. (d) HRTEM image of CuS NCs obtained with precursor S:Cu ratio of 2:1. (e-f) Experimental XRD patterns (e) and optical spectra (f) of the corresponding NCs. For comparison, the standard XRD patterns of covellite (JCPDS No. 00-006-0464), spionkopite ($\text{Cu}_{39}\text{S}_{28}$, JCPDS No. 00-036-0380) and monoclinic low chalcocite (Cu_2S , JCPDS

No. 01-083-1462) are also reported in panel e). The starting TGA:Cu ratio for all the syntheses is 1:1.

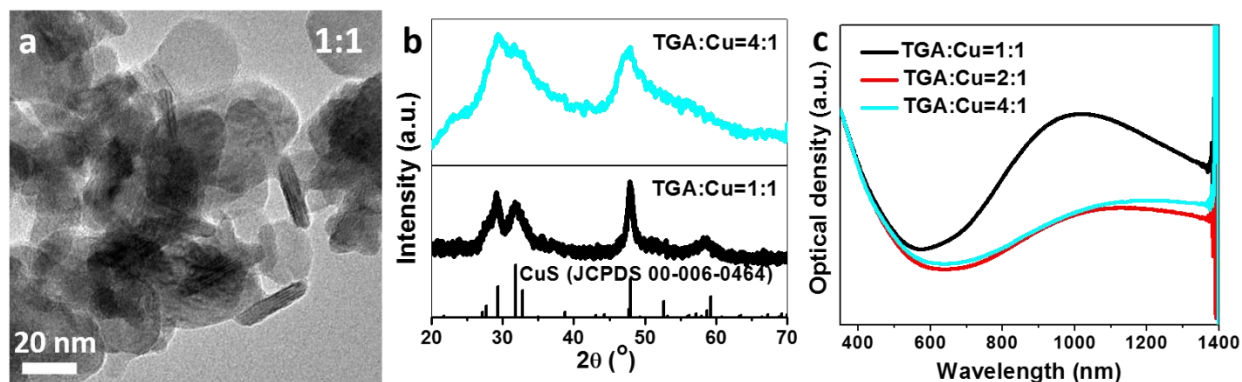


Fig. S7 TEM image (a) of CuS NCs, XRD patterns (b) and optical absorption (c) of Cu_{2-x}S NCs synthesized with different TGA:Cu ratios. The precursor S:Cu ratio is 2:1 and the reaction time is 2 h.

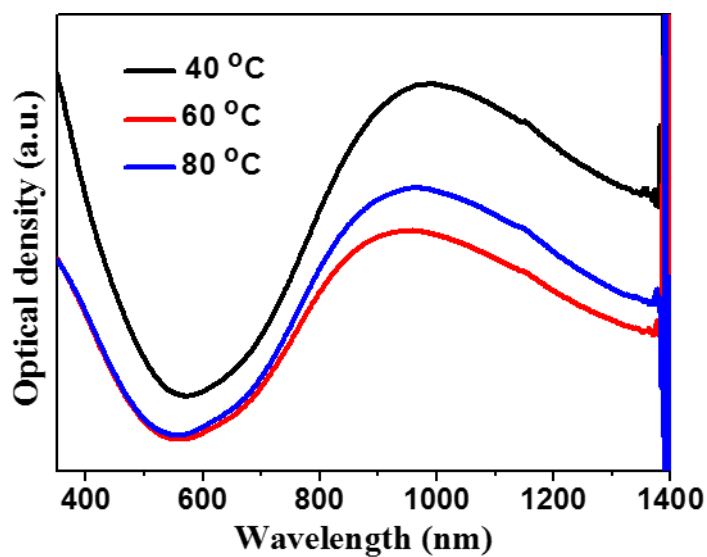


Fig. S8 Optical spectra of Cu_{2-x}S NCs collected at different reaction temperatures, in the presence of TGA. The precursor S:Cu ratio is 2:1 and the reaction time is 4 h.

3. Characterization of Cu_{2-x}S NCs achieved by reacting CuCl_2 with Na_2S in the presence of GSSG or GSH as ligand

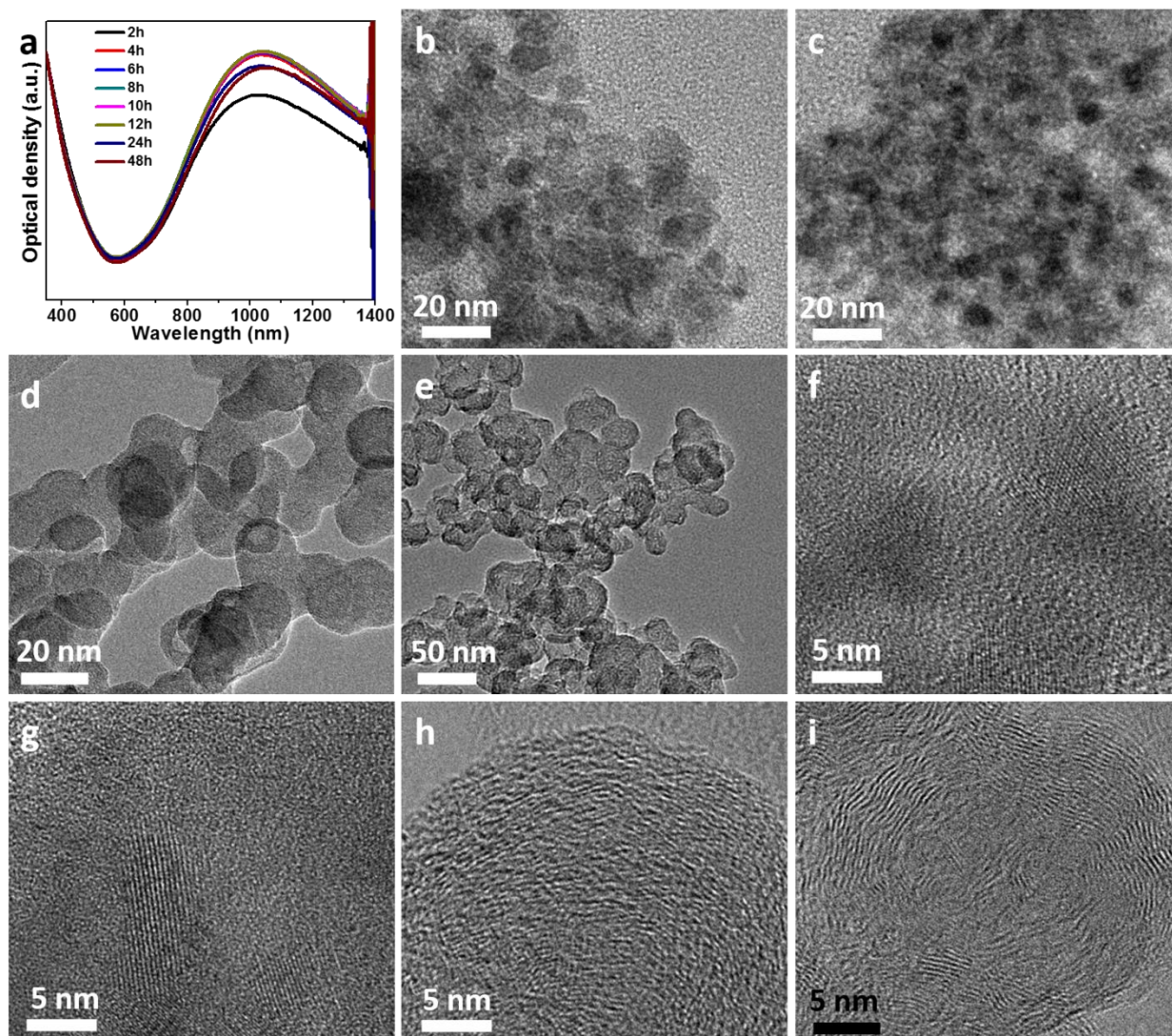


Fig. S9 (a) Optical absorption spectra of CuS NCs collected at different reaction time as dictated, by reacting CuCl_2 with Na_2S in the presence of GSSG. (b-e) TEM images of CuS NCs collected at 1 h (b), 4 h (c), 8 h (d) and 24 h (e). (f-i) HRTEM images of CuS NCs collected at 1 h (f), 4 h (g), 8 h (h) and 24 h (i).

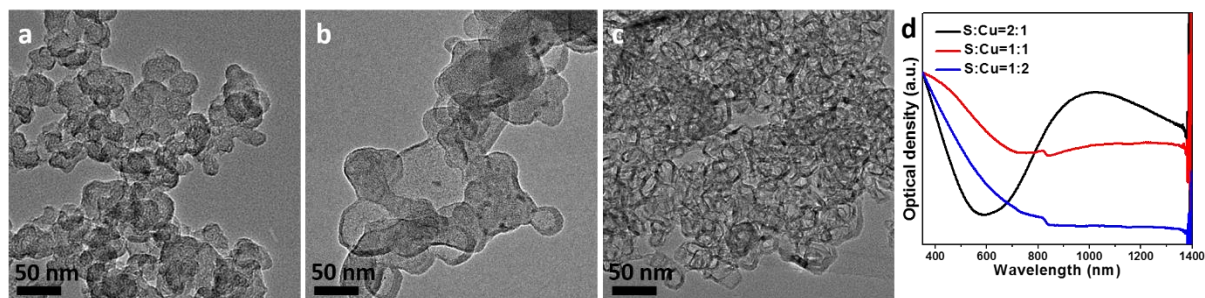


Fig. S10 (a-c) Representative TEM images $Cu_{2-x}S$ NCs achieved with precursor S:Cu ratios of 2:1 (a), 1:1 (b) and 1:2 (c) in the presence of GSSG ligand. (d) Optical spectra of the corresponding NCs collected with different precursor S:Cu ratios as dictated.

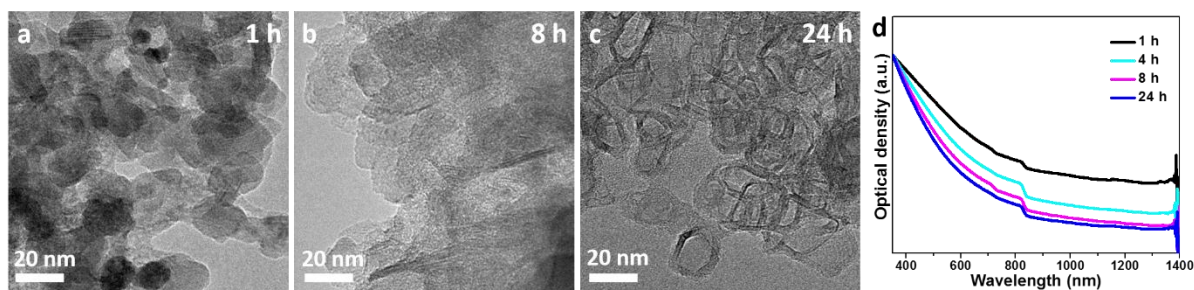


Fig. S11 TEM images (a-c) and optical absorption (d) of $Cu_{2-x}S$ NCs collected at different reaction time as dictated, in the presence of ligand GSSG by S:Cu=1:2.

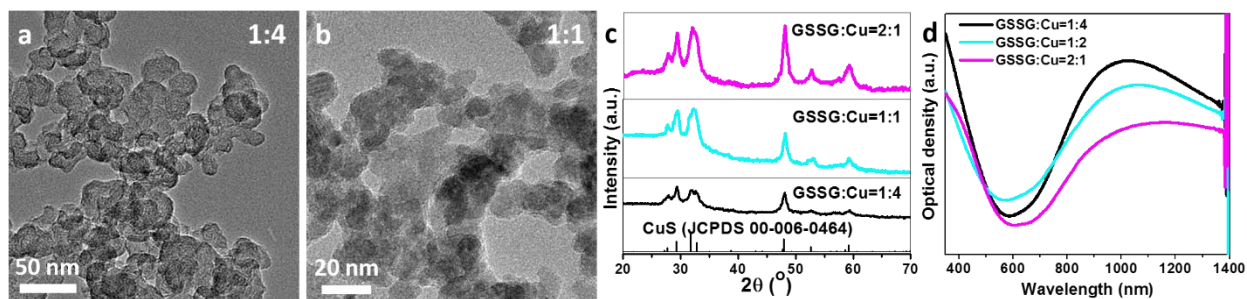


Fig. S12 TEM images (a-b), XRD patterns (c) and optical absorption (d) of $Cu_{2-x}S$ NCs synthesized with different precursor GSSG:Cu ratios by S:Cu=2:1.

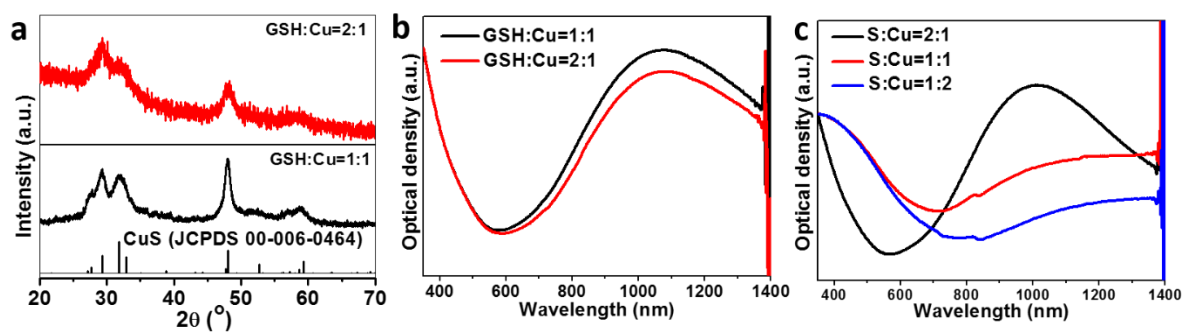


Fig. S13 (a-b) XRD patterns (a) and optical absorption spectra (b) of the Cu_{2-x}S NCs synthesized with different GSH:Cu ratios. (c) Optical absorption spectra of Cu_{2-x}S NCs collected with different precursor S:Cu ratios as dictated.

4. Cu_{2-x}S NCs achieved by reacting $\text{Cu}(\text{NO}_3)_2$ with Na_2S in the presence of various ligands

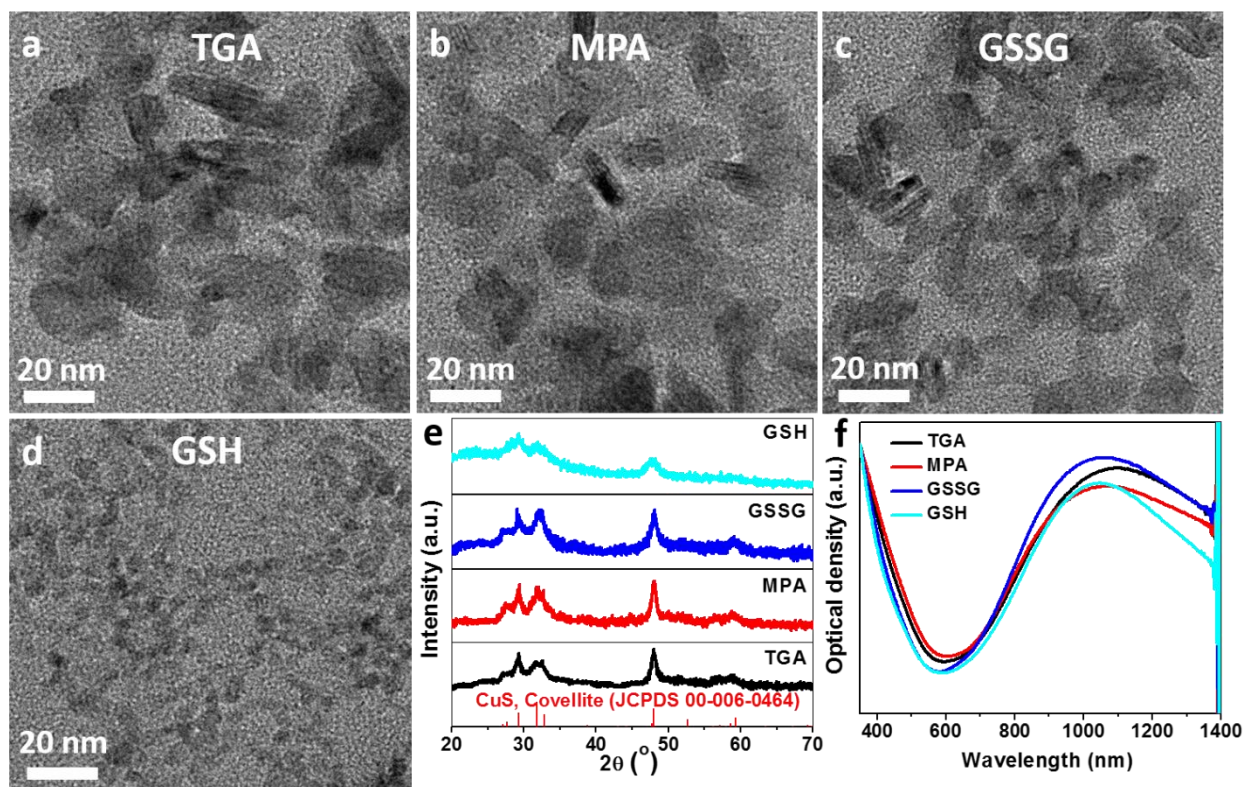


Fig. S14 TEM images (a-d), XRD patterns (e) and optical spectra (f) of CuS NCs achieved by reacting $\text{Cu}(\text{NO}_3)_2$ with Na_2S , in the presence of different ligands as dictated.

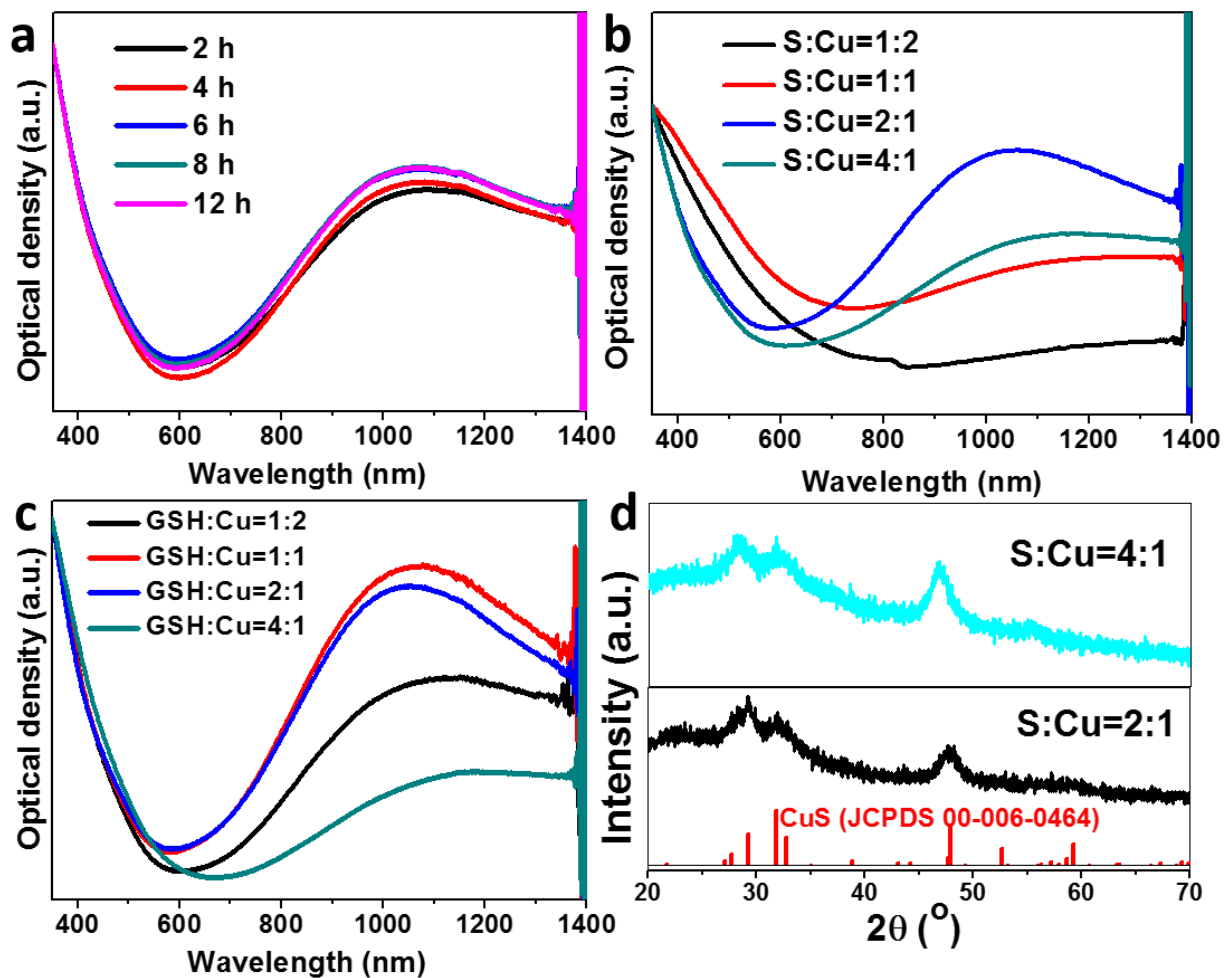


Fig. S15 Optical spectra (a-c) and XRD patterns (d) of various Cu_{2-x}S NCs obtained by reacting $\text{Cu}(\text{NO}_3)_2$ with Na_2S , in the presence of GSH under different conditions as dictated.

5. XRD patterns and optical spectra of CuS NCs collected by reacting various copper precursors with $(\text{NH}_4)_2\text{S}$

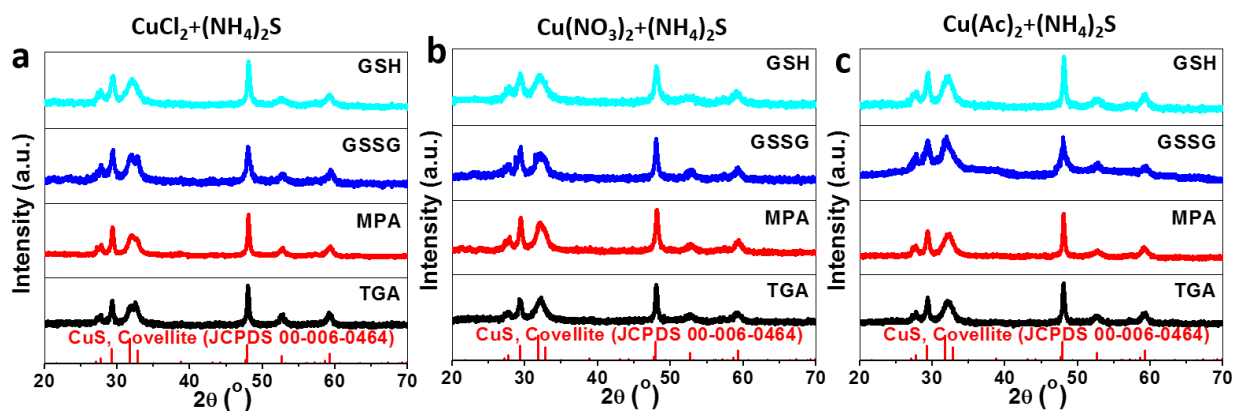


Fig. S16 XRD patterns of the CuS NCs obtained by reacting various copper precursors with $(\text{NH}_4)_2\text{S}$, in the presence of different ligands as dictated.

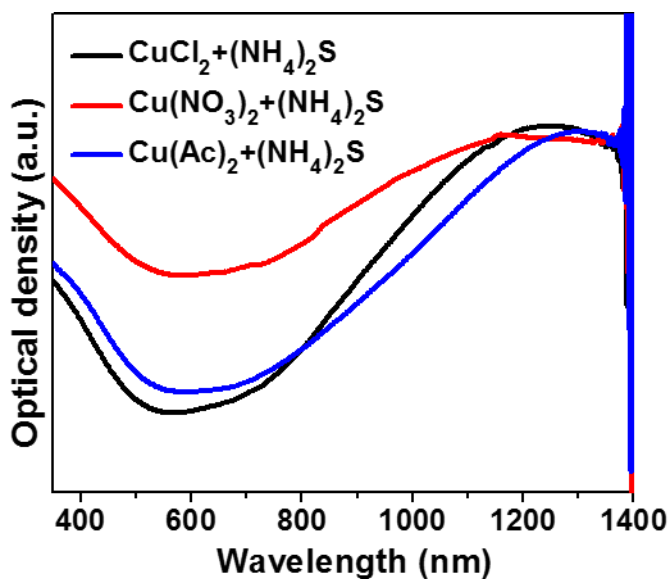


Fig. S17 Optical spectra of the CuS NCs obtained by reacting various copper precursors with $(\text{NH}_4)_2\text{S}$, in the presence of GSH.

6. Gram-scale synthesis of CuS NCs

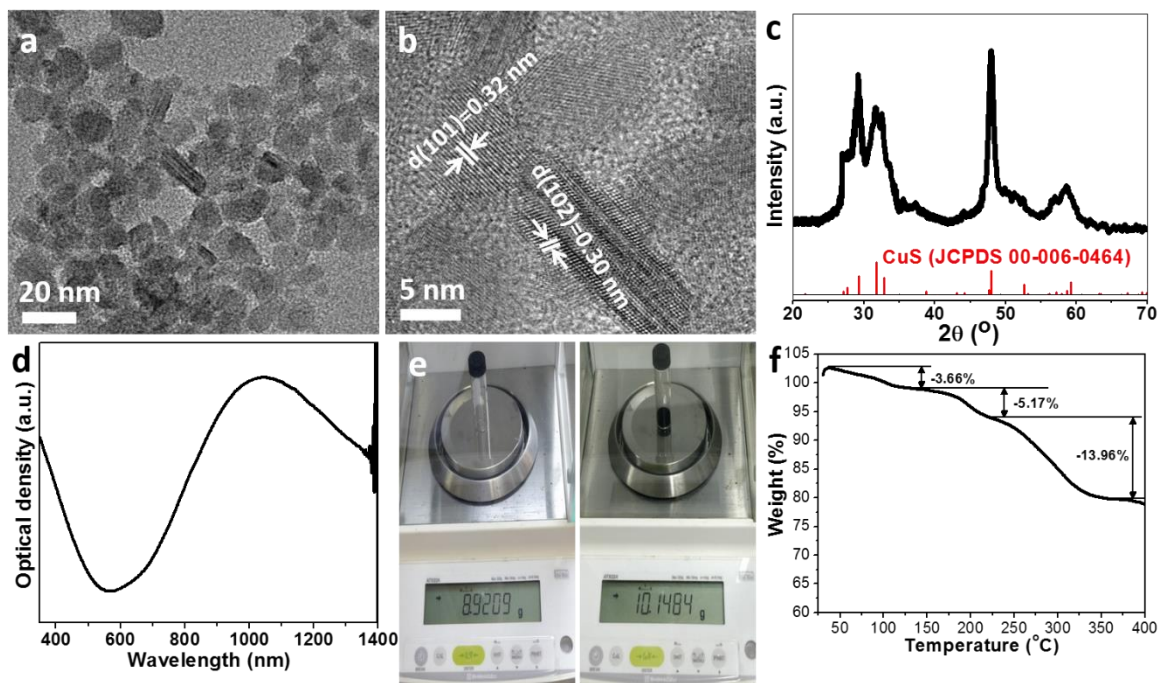


Fig. S18 TEM image (a), HRTEM image (b), XRD pattern (c), optical absorption (d), weighing measurement (e) and TGA analysis (f) of the CuS NCs achieved by gram-scale synthesis by MPA as ligand.

7. Photothermal performance of Cu_{2-x}S NCs

The photothermal conversion efficiency (PCE, η) of Cu_{2-x}S NCs was calculated according to the previous method.¹ The η value was calculated as follows.^{1, 2}

$$\eta = \frac{hS(T_{\max} - T_{\text{surr}}) - Q_{\text{dis}}}{I(1 - 10^{-A_\lambda})} \quad (1)$$

Where h is the heat transfer coefficient, S is the surface area of the container, and the value of hS was obtained from Fig. 6f. The maximum system temperature (T_{\max}) under irradiation was 51.5 °C, the surrounding temperature (T_{surr}) was 22 °C, and ($T_{\max} - T_{\text{surr}}$) is 29.5 °C according to Fig. 5e. The laser powder I is 72 mW, and the absorbance of CuS NCs at 806 nm is 1.631 (A_λ). Q_{dis} is the rate of heat input due to light absorption by the solvent.

To obtain hS , a parameter θ is introduced as followed:

$$\theta = \frac{T - T_{\text{surr}}}{T_{\max} - T_{\text{surr}}} \quad (2)$$

The system time constant (τ_s) can be calculated by using Eq. 3,³ which was estimated to be 257.90 s by applying the linear time data according to Fig. 6f in the main text.

$$t = -\tau_s L_n(\theta) \quad (3)$$

$$hS = \frac{m_{\text{H}_2\text{O}} C_{\text{H}_2\text{O}}}{\tau_s} \quad (4)$$

The value of hS is derived according to Eq 4, where τ_s is the sample system time constant, $m_{\text{H}_2\text{O}}$ and $C_{\text{H}_2\text{O}}$ are the mass (3 g) and heat capacity (4.2 J·g⁻¹·°C⁻¹) of solvent (deionized water), respectively. According to Eq 4, hS was calculated to be 48.856 mW/°C.

$$Q_{\text{dis}} = hS(T_{\text{H}_2\text{O},\max} - T_{\text{H}_2\text{O},\text{surr}}) \quad (5)$$

Q_{dis} is the rate of heat input due to light absorption by the solvent. The maximum solvent (H₂O) temperature ($T_{\text{H}_2\text{O},\max}$) under irradiation was 22.3 °C, the surrounding temperature ($T_{\text{H}_2\text{O},\text{surr}}$) was 22 °C, and ($T_{\text{H}_2\text{O},\max} - T_{\text{H}_2\text{O},\text{surr}}$) was 0.3 °C. So the Q_{dis} was measured to be 14.6568 mW from the Eq. 5.

Thus, replacing corresponding values of each parameter in Eq. 1, the η value of the CuS NCs can be calculated to be 20.3%.

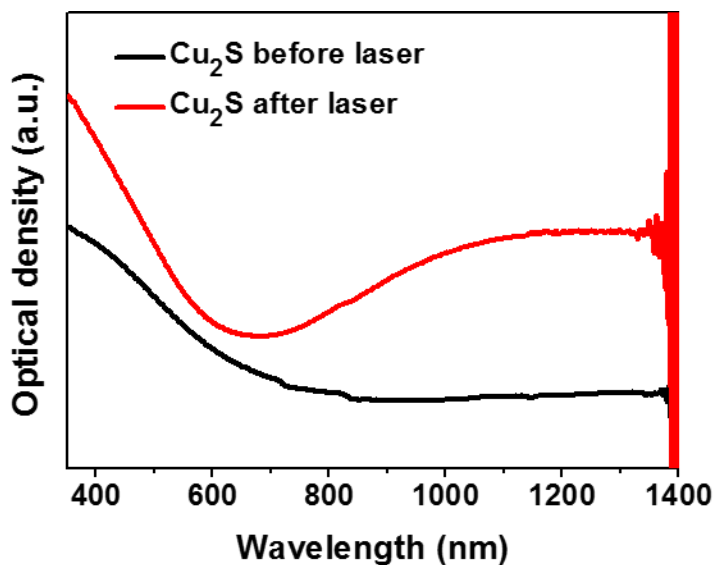


Fig. S19 Optical absorption spectra of the Cu₂S NCs before (black curve) and after (red curve) photothermal test.

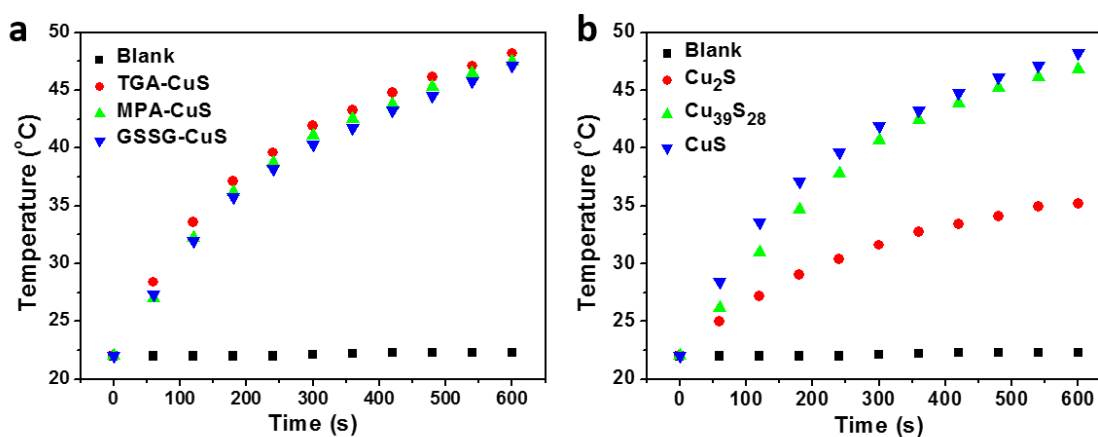


Fig. S20 (a) Temperature increment of CuS NCs (1.4 mM) synthesized by different capping ligands as dictated, under 806 nm laser irradiation at 1.2 W/cm². (b) Temperature increment of various Cu_{2-x}S NCs (1.4 mM) collected with different precursor S:Cu molar ratios.

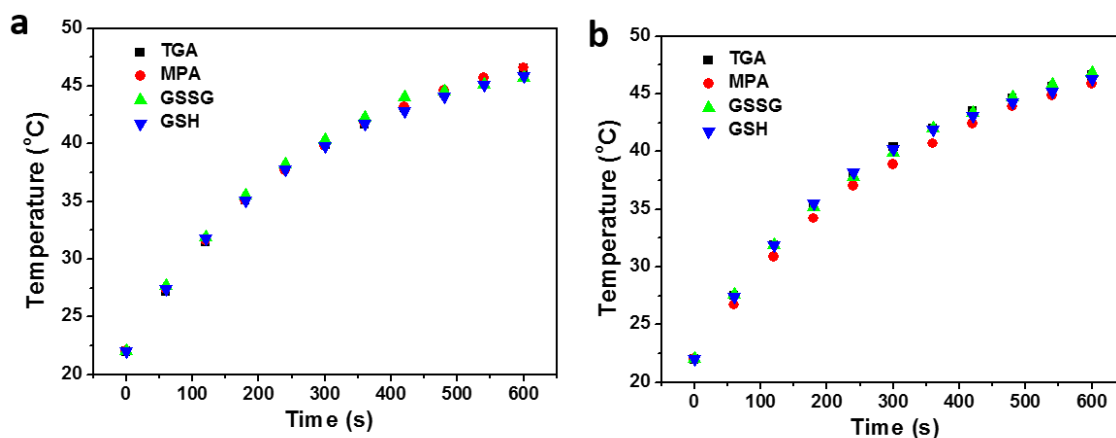


Fig. S21 (a-b) Temperature increment of CuS NCs (1.4 mM) synthesized by reacting Cu(NO₃)₂ (a), and Cu(Ac)₂ (b) with Na₂S in the presence of different ligands as dictated.

Fig. S20 and S21 provide the temperature increment of dispersions with various CuS and Cu_{2-x}S NCs, respectively, under 806 nm laser irradiation (1.2 W/cm²). There no obvious difference in temperature increment of CuS NCs synthesized by TGA, MPA, and GSSG as ligand, respectively (Fig. S20a). The temperature of the solutions containing Cu₂S, Cu₃₉S₂₈, and CuS NCs was raised by 13.2 °C, 24.8 °C, 26.2 °C in 600 s, respectively (Fig. S20b). Compared with Cu₃₉S₂₈ and Cu₂S NCs, the higher photothermal conversion of CuS NCs is due to the stronger localized surface plasmon resonances which originated from the abundant Cu vacancies. The CuS NCs collected by reacting Cu(NO₃)₂ and Cu(Ac)₂, respectively, with Na₂S in the presence of different ligands display almost the same temperature increment under the same photothermal conditions (Fig. S21).

References

1. Q. Tian, F. Jiang, R. Zou, Q. Liu, Z. Chen, M. Zhu, S. Yang, J. Wang, J. Wang and J. Hu, *ACS Nano*, 2011, **5**, 9761-9771.
2. X. Bu, D. Zhou, J. Li, X. Zhang, K. Zhang, H. Zhang and B. Yang, *Langmuir*, 2014, **30**, 1416-1423.
3. A. Riedinger, T. Avellini, A. Curcio, M. Asti, Y. Xie, R. Tu, S. Marras, A. Lorenzoni, S. Rubagotti, M. Iori, P. C. Capponi, A. Versari, L. Manna, E. Seregni and T. Pellegrino, *J. Am. Chem. Soc.*, 2015, **137**, 15145-15151.